Particle densities for three hollow cathode discharge configurations

S.E. Acosta[1], V. Aboites, S. Chávez[2], H. Sánchez, D. Iturbe[3]

Laboratorio de Láseres
Centro de Investigaciones en Optica
Apartado postal 948, 37000 León, Gto.

Recibido el 26 de septiembre de 1991; aceptado el 14 de enero de 1992

Abstract. We report helium-ion, copper-ion, and copper-atom densities for three different hollow cathode laser configurations: quadrupolar, helicoidal and slotted. These results were obtained at different buffer gas pressures and current densities from measurements of the spontaneous emission of single ionized copper atoms. The particle densities were obtained by fitting the experimental data with a balance equation model taking into account the discharge current density, the pressure and electronic and ionic temperature dependence of the buffer ion, metal and metal ion diffusion times.

Resumen. Reportamos densidades de iones de helio, iones de cobre y átomos de cobre para tres diferentes configuraciones láser de cátodo hueco: cuadrupolar, helicoidal y de ranura. Estos resultados fueron obtenidos de mediciones de la emisión espontánea de átomos de cobre ionizados. Las densidades de partículas fueron obtenidas ajustando los datos experimentales con un modelo de ecuación de balance que toma en cuenta para la evaluación de los tiempos de difusión de los iones de gas, iones de metal y átomos de metal, la dependencia de la densidad de corriente de descarga, la presión y la temperatura electrónica y iónica del gas.

PACS: 52.70.Kz; 52.70.Nc; 52.80.Vp

1. Introduction

Although the first laser transitions using hollow cathode excitation were reported in 1970 by Karabut [1], Sugawara [2], and Schuebel [3], there is yet now a great deal of interest to find new configurations in order to improve the efficiency of this kind of lasers [4]. As is well known, some of the principal characteristics of hollow cathode metal ion lasers are their ability to create significant metal density via sputtering [5] and their possibility of operation in the UV (220–320 nm) at one-twentieth the discharge current required for rare-gas ion lasers [6]. Nevertheless, an important feature of metal ion lasers for optimal operation is their need to achieve high enough metal ion densities. As it is known the metal ion density for similar current and pressure conditions strongly depends on the geometrical configuration of the hollow cathode.

---

[1]On leave at: University College of Swansea, U.K.
[2]Present address: Imperial College, U.K.
[3]Present address: INAOE, Puebla, México.

In this paper, we report some of the plasma characteristics of three hollow cathode copper ion lasers, namely: quadrupolar (to our knowledge, not previously reported), helicoidal and slotted. Hollow cathode discharges were produced using helium as the buffer gas and copper as the metal cathode. In particular the helium-ion, copper-ion and copper-atom density as a function of the current density for several buffer gas pressures were calculated. In order to obtain the particle densities, we measured the intensity of spontaneous emission and fitted our data with a balance equation model in which it is assumed that the principal mechanism of creation of metal atoms is via sputtering from metal and buffer ions, whereas the principal mechanism of metal atom loss are diffusion to the walls and recombination of the particles there (*i.e.* ambipolar diffusion), and the charge-transfer reaction:

$$He^+ + Cu \longrightarrow He + (Cu^+)^* + \Delta E, \tag{1}$$

where He, He^+, Cu and $(Cu^+)^*$ represent the buffer gas atom, buffer gas ion, metal atom and metal ion in an excited energy state, respectively. ΔE is the energy difference between He^+ and $(Cu^+)^*$.

By fitting the experimental results with the balance equation model we managed to obtain the sputtering coefficient for copper ions as a function of the buffer gas pressure. In this way we were able to calculate the buffer ion density, metal ion density and metal atom density.

2. THEORY

The basis for the mathematical derivation of the current dependent densities [7], are three balance equations involving the spatial averaged copper atom, copper ion and helium ion densities:

a) Copper atom equation balance:

$$\xi_{Cu^+}\frac{N_{Cu^+}}{\tau_{Cu^+}} + \xi_{He^+}\frac{N_{He^+}}{\tau_{Cu^+}} = \frac{N_{Cu}}{\tau_{Cu}} + K N_{Cu} N_{He}, \tag{2}$$

where the left-hand side represents the main metal atom production mechanism, that is; the sputtering action of copper and buffer gas ions, while on the right-side the dominant loss mechanisms are involved; the copper vapor diffusion back to the cathode and the loss due to the charge transfer reaction (1). ξ_i, N_i and τ_i ($i = Cu^+$, He^+, Cu) represent the sputtering coefficients due to the i-ions, particle densities and diffusion times, respectively, and K is the charge transfer constant.

b) Copper ion balance equation:

$$K N_{Cu} N_{He^+} = \frac{N_{Cu^+}}{\tau_{Cu^+}} \propto \Phi_{SE}, \tag{3}$$

where the left-hand side represents the copper ion creation mechanism due to the charge transfer reaction (1) and the right-hand side involves the copper ion loss due to the ambipolar diffusion. Φ_{SE} is the intensity of the spontaneous emission of lines from dominantly

charge transfer populated energy levels and is directly proportional to the charge transfer rate, hence this intensity is a measure of N_{Cu^+}/τ_{Cu^+} provided a correct scaling is made.

c) Balance equation for the particle current densities at the cathode surface:

$$J = e[\Gamma_e + \Gamma_{Cu^+} + \Gamma_{He^+}], \tag{4}$$

where Γ_i ($i = e$, Cu^+, He^+) are electron, copper ion, and helium ion flow densities respectively, at the cathode surface.

The electron flow density is related to the ion flow densities via

$$\Gamma_e = \gamma_{Cu^+}\Gamma_{Cu^+} + \gamma_{He^+}\Gamma_{He^+}, \tag{5}$$

here, γ_i ($i = Cu^+$, He^+) are the secondary electron emission coefficients due to ion collisions at the cathode surface.

Because of the fact that the production of electron-ion pairs is almost uniform in the glow volume [7] and the ambipolar diffusion is the dominant loss mechanism at the cathode surface, particle densities can be related to the flow densities at the cathode by

$$\frac{\Gamma_i A}{V_0} = \frac{N_i}{\tau_i}, \tag{6}$$

where A is the cathode surface, V_0 is the glow region volume and $i = Cu^+$, He^+.

Equations (2)–(6) combined yield three coupled equations that can be solved in order to obtain the particle densities N_{He^+}, N_{Cu^+} and N_{Cu} as a function of the current density J,

$$N_{He^+} = \frac{-\left(c_1 + \frac{c_2\tau_{He^+}}{eF}J\right) + \left[\left(c_1 + \frac{c_2\tau_{He^+}}{eF}J\right)^2 + 4(c - c_1c_2)\left(\frac{\tau_{He^+}}{eF}J\right)\right]^{1/2}}{2(c - c_1c_2)}, \tag{7a}$$

$$N_{Cu^+} = \frac{N_{He^+}^2\tau_{Cu}\tau_{Cu^+}\xi_{He^+}K}{\tau_{He^+}(1 - c_2N_{He^+})}, \tag{7b}$$

$$N_{Cu} = \frac{N_{Cu^+}}{K\tau_{Cu^+}N_{He^+}}, \tag{7c}$$

where

$$c = K\tau_{Cu}\xi_{Cu^+}(1 + \gamma_{Cu^+}), \quad c_1 = 1 + \gamma_{He^+}, \quad c_2 = K\tau_{Cu}.$$

The diffusion times depend on the diffusion coefficients through [8],

$$\tau_i = \left(\frac{r}{2.405}\right)^2 \frac{1}{D_i} \tag{8a}$$

for a cylindrical configuration, and

$$\tau_i = \left(\frac{2a}{\pi}\right)^2 \frac{1}{D_i} \tag{8b}$$

for a slotted configuration. Here r is the radius of the glow region and $2a$ is the cathode surface separation in a cylindrical and slotted configuration, respectively.

The ion diffusion coefficients depend on the electron and ion temperatures as well as on the ion mobilities through [9]

$$D_i = \frac{k}{e}(T_e + T_i)\mu_i, \tag{9}$$

where k is the Boltzmann's constant and e is the electron charge.

As it was experimentally showed by McNeil's *et al.* [10] electron and ion temperatures depend on the current density. Extrapolating their results we considered this dependence through

$$T_e(J) = 11600(0.3221J + 0.063), \tag{10}$$

$$T_i(J) = 1500 - 962\exp\left(\frac{-J}{0.218}\right). \tag{11}$$

The experimental temperature was taken to be equal to the ion temperatures, and the buffer gas pressure dependence of the ion mobility was also taken into account via [11]

$$\mu_i = \frac{760\ (0.75)T\ [°\mathrm{K}]}{P\ [\mathrm{hPa}]\ 273}\mu_r, \tag{12}$$

where $\mu_r = 10.4$ for He^+ and $\mu_r = 21.0$ for Cu^+ [9], $i = He^+, Cu^+$.

For copper atoms, the diffusion coefficient is given by [11]

$$D_{Cu} = \frac{0.126}{P\ [\mathrm{hPa}]}T^{3/2}. \tag{13}$$

Other quantities were taken as constants on the basis of previous references: the secondary electron emission coefficient $\gamma_i = 0.2$ electrons per ion [7] ($i = He^+, Cu^+$), the charge transfer rate constant $K = 2 \times 10^{-9}$ cm^3 sec^{-1} [12], and the helium ion sputtering coefficient $\xi_{He^+} = 0.02$ atoms per ion [7,11,12]. The sputtering coefficient due to copper ions ξ_{Cu^+} was taken as a fitting parameter between theory and experimental data for several buffer gas pressures. As it is known [7] sputtering metal ion lasers should be operated with $\xi_{Metal+} > 1$ while hollow cathode gas lasers (*i.e.* He–Ne, Ar^+, etc.) with

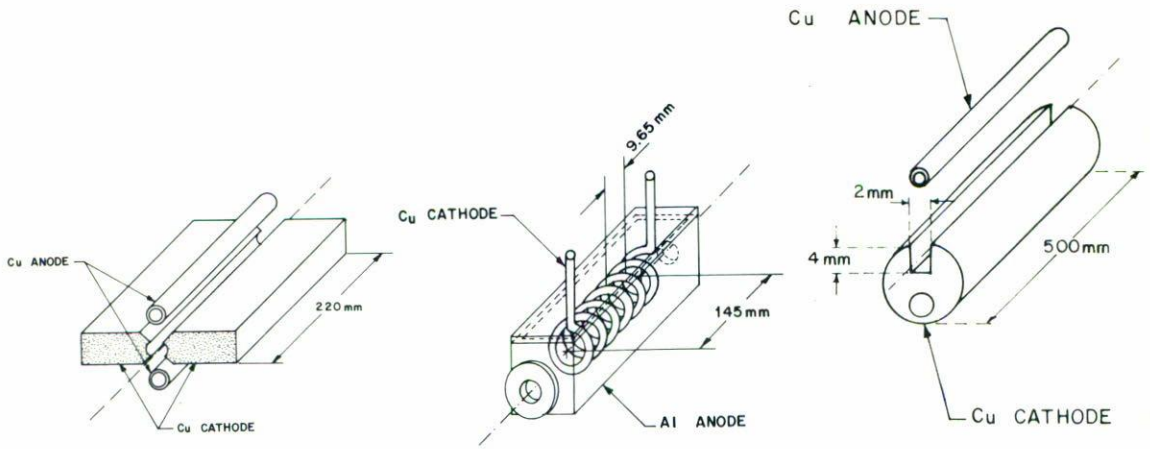

FIGURE 1. Hollow cathode configurations used. a) Quadrupolar. b) Helicoidal. c) Slotted.

TABLE I.

Configuration	A (cm^2)	V_0 (cm^3)	
Quadrupolar	27.76	6.65	$r = .325$ cm
Helicoidal	19.78	4.1	$r = .3$ cm
Slotted	60.0	5.0	$a = 1$ cm

$\xi_{\text{Metal}+} < 1$. The values obtained for this coefficient as a function of the helium pressure are shown in Table II.

3. EXPERIMENT AND RESULTS

A scheme of the three configurations employed is shown in Fig. 1. Their main characteristics are shown in Table I. As can be seen from Eq. (3), using the experimental results of Φ_{SE} *vs.* J and the model described in the previous section with an appropriate value for the sputtering coefficient ξ_{Cu^+}, it is possible to fit the model to the experimental results. Fig. 2 shows this fitting for the case of the quadrupolar configuration for different helium pressures and Table II resumes the values obtained for this coefficient. Since the sputtering coefficient does not depends on the geometry of the discharge but on the buffer gas and cathode metal used, the same values were obtained when fitting the experimental results of the helicoidal and the slotted configuration. The measurement of Φ_{SE} was done

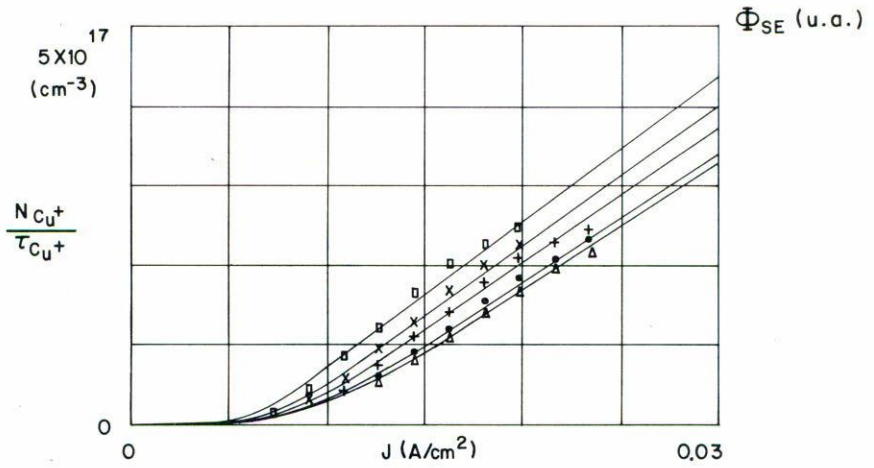

FIGURE 2. Example of the fitting of the experimental (symbols) and theoretical (solid lines) results obtained for the spontaneous emission intensity, which is directly related to the copper ion loss rate versus current density for five buffer gas pressures for the quadrupolar configuration. Symbols represent different helium pressures: □ 3.8 hPa, × 4.4 hPa, + 4.8 hPa, • 5.4 hPa and Δ 5.6 hPa.

TABLE II. Sputtering coefficients for a He–Cu hollow cathode discharge obtained from our measurements and fitting to the balance equation model.

Buffer gas pressure (hPa)	ξ_{Cu^+} (atom/ion)
3.4	2.8
4.4	2.16
4.8	1.88
5.4	1.64
5.6	1.54

using a 1870 SPEX spectrometer which was used as a monochromator to observe a single wavelength which was detected using a linear amplifier and a photodiode. In all cases the spontaneous emission Φ_{SE} was observed for the 501.26 nm line of Cu II.

Figs. 3, 4 and 5 summarize the results obtained for the particle densities in the quadrupolar, helicoidal and slotted configuration. As it has been observed by other authors [7], the copper ion loss rate decreases as buffer gas pressure increases, contrary to the behavior observed for the pressure dependence of the laser output power [6,13] in which, for low pressures (up to about 14 torr) the intensity increases as the pressure increases for a constant current density, while for higher pressures the intensity decreases as buffer gas pressure increases. This difference in pressure dependence for spontaneous and stimulated emission has been explained by Koch and Eichler [7] as an indication that the lower laser levels are not solely populated by the spontaneous emission from the upper laser level but additional population of the lower laser levels via different channels must be considered.

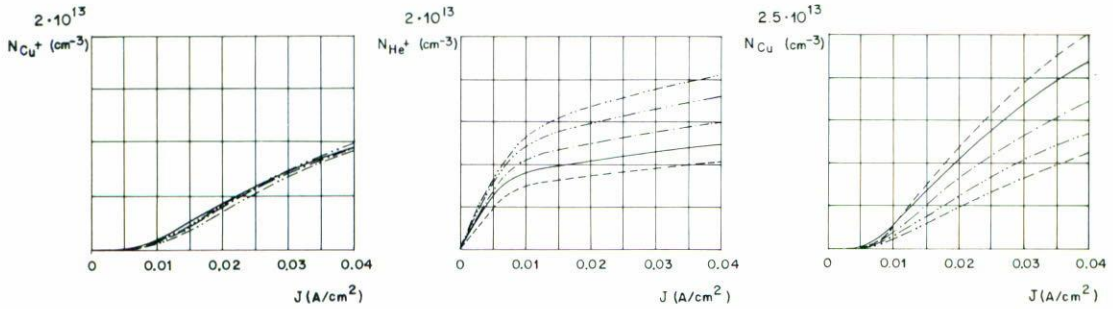

FIGURE 3. Particle densities *versus* current density calculated for the quadrupolar configuration by taking into account the experimental conditions and the values of the sputtering coefficients shown in Table II. a) Copper ion density, b) Helium ion density and c) Copper atom density. Symbols represent different helium pressures: - - - 3.4 hPa, — 4.4 hPa, —·— 4.8 hPa, —··— 5.4 hPa, — —·— — 5.6 hPa.

Figs 3, 4 and 5 show the calculated copper ion, helium ion and copper density. From Figs. 3-a, 4-a and 5-a we can see that the quadrupolar configuration produced the larger density of copper ions per unit volume followed by the helicoidal and the slotted configuration. The copper ion density in this last one geometry was two orders of magnitude smaller surely due to the smaller current density achieved. Nevertheless, in all cases the experimental results are consistent with the predictions of the model used. It is seen from Eq. (3) and relation (1) that the copper ion production is directly proportional to helium ion and copper density which are shown in Figs. 3-b-c, 4-b-c and 5-b-c.

We should point out that even though the larger total copper ion density was obtained for the quadrupolar configuration, the helicoidal one was more efficient in relation to the fact that the cathode area in this case was 1.4 times smaller than in the quadrupolar one.

4. CONCLUSIONS

In conclusion, by using a simple model which takes into account pressure and electron and ion temperature dependence of the diffusion coefficients and diffusion times, and measuring only the spontaneous emission from hollow cathode discharges, we could obtain

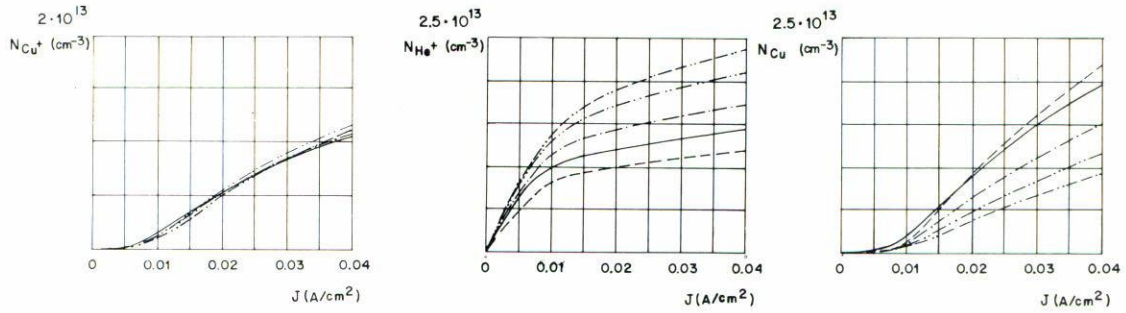

FIGURE 4. Particle densities versus current density calculated for the helicoidal configuration by taking into account the experimental conditions and the values of the sputtering coefficients shown in Table II. a) Copper ion density, b) Helium ion density and c) Copper atom density. Symbols represent different helium pressures: - - - 3.4 hPa, — 4.4 hPa, —·— 4.8 hPa, —··— 5.4 hPa, — —·— — 5.6 hPa.

the main plasma characteristics. It was also possible to evaluate the metal ion sputtering coefficient as a function of buffer gas pressure. We obtained this coefficient at five pressures taking care of same values were obtained for the three configurations as these coefficients must be independent on the hollow cathode configuration. Even though our experimental pressure and current density range was rather small, a significant variation on the values of the copper ion sputtering coefficient was obtained.

From the three hollow cathode geometries studied the quadrupolar one produced the higher total copper ion density per unit volume followed by the helicoidal and the slotted one. However, since the cathode area of the helicoidal configuration is 1.4 times smaller than the quadrupolar one, we may conclude that this last configuration may be more efficient for a laser application.

ACKNOWLEDGMENTS

Technical assistance from M.C.A. Melchor and Ing. C. Aguilera is sincerely acknowledged as well as suggestions and comments from Dr. J. de la Rosa, Dr. E. Landgrave and M. Sc. R. Flores.

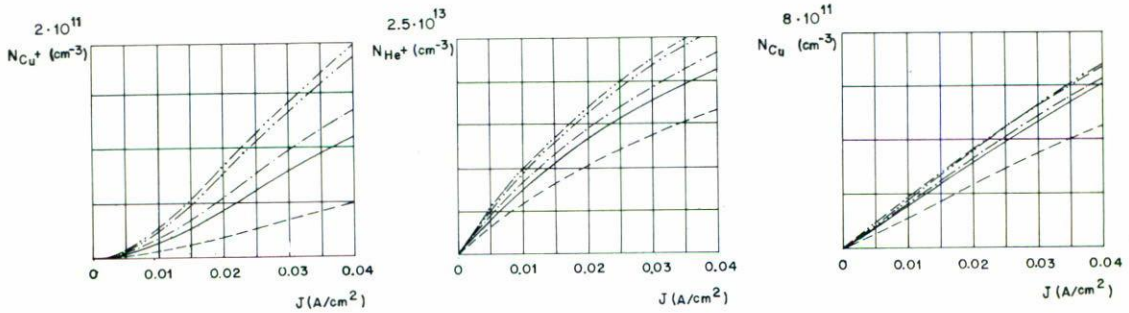

FIGURE 5. Particle densities versus current density calculated for the slotted configuration by taking into account the experimental conditions and the values of the sputtering coefficients shown in Table II. a) Copper ion density, b) Helium ion density and c) Copper atom density. Symbols represent different helium pressures: - - - 3.4 hPa, — 4.4 hPa, —·— 4.8 hPa, —··—·· 5.4 hPa, — —··— — 5.6 hPa.

REFERENCES

1. E. K. Karabur *et al.*, *Sov. Phys. Tech. Phys.* **14** (1970) 1447.
2. Y. Sugawara and V. Tokiwa, *Jap. J. Appl. Phys.* **9** (1970) 588.
3. W. K. Schuebel, *Appl. Phys. Lett.* **16** (1970) 470.
4. P. Mezei, P. Apai, M. Jánossy and K. Rózsa, *Opt. Comm.* **78** (1990) 259.
5. F.J. de Hoog *et al.*, *J. Appl. Phys.* **48** (1977) 3701.
6. D. C. Gerstenberger *et al.*, *J.Q.E.* QE-10 (8) (1980) 820.
7. H. Koch and H. J. Eichler, *J. Appl. Phys.* **54** (1983) 4939.
8. E. Mc.Daniel, E. A. Mason, *The Mobility and Diffusion of Ions in Gases*, John Wiley, N.Y. (1973).
9. E. Mc. Daniel, *Collision Phenomena in Ionized Gases*, John Wiley, N.Y. (1979).
10. J.P. McNeil G.J. Collins and F.J. de Hoog, *J. Appl. Phys.* **50** (1979) 6183.
11. J.M. de la Rosa, *Vergleich der Eigenschaften geschlitzter und zylindrischer Hohlkathoden in Cu-II Laser*, Jahresarbeit am Optischen Institut der Technischen Universität Berlin (1983).
12. B.E. Warner and K.B. Persson, *J. Appl. Phys.* **50** (1979) 5694.
13. H.J. Eichler *et al.*, *Appl. Phys. B* **26** (1981) 49.
14. G. Bekefi, *Principles of Laser Plasmas*, Wiley Interscience (1976) 555.